J. Phys. B: At. Mol. Opt. Phys. **23** (1990) 1005–1016. Printed in the UK

Differential cross sections for elastic positron–H_2 collisions using the *R*-matrix method

Grahame Danby† and Jonathan Tennyson

Department of Physics and Astronomy, University College London, London WC1E 6BT, UK

Received 26 June 1989, in final form 4 December 1989

Abstract. Results are presented for positron–H_2 collision cross sections for energies below the positronium formation threshold. Calculations are performed with a variety of target representations, including full configuration interaction within a basis of Slater-type orbitals, and several models. The most sophisticated model includes the use of pseudo-excited electronic states of the target to account for intermediate-range polarisation effects. Short- and long-range polarisation effects are also considered. Calculations are performed for $\Sigma_g^+, \Sigma_u^+, \Pi_u, \Pi_g, \Delta_g$ and Δ_u symmetries which are combined to give differential cross sections as a function of energy. These calculations underestimate the Σ_g^+ eigenphase sum but perform better for the higher symmetries. The differential cross sections show a minimum for angles about 45° which should be amenable to experiment. A computationally more efficient reformulation of the positron–molecule scattering problem is presented within the *R*-matrix method. Corrections are given for some previously published results.

1. Introduction

The study of the interaction of positrons with atoms and molecules has become an increasingly popular area of study due, at least in part, to the increased availability of positron beams (Charlton 1985). This experimental activity has encouraged a number of workers to perform calculations on these systems. In particular several methods have been developed to consider low-energy positron–molecule collisions from first principles. These methods have recently been the subject of both comprehensive and short reviews by Armour (1988, 1989). In these works Armour pays particular attention to the status of positron–hydrogen molecule collision calculations, a subject he himself has worked on for a number of years (see, for example, Armour 1985, Armour and Baker 1987, Armour *et al* 1989).

There is little information on differential cross sections for positron–atom or molecule collisions. Campeanu (1977) and Humberston (1979) calculated low-energy differential cross sections for the e^+–He system which show a pronounced energy-dependent structure below the positronium formation threshold. Similar structures have been predicted for e^+–alkali-atom collisions (Ward *et al* 1988, 1989). Measurements have been performed on e^+–Ar which have yet to fully resolve this low-energy structure (Kauppila and Stein 1987).

---

† Present address: Department of Physics and Astronomy, University of Oklahoma, Norman, OK 73019, USA.

0953-4075/90/061005+12$03.50

The molecular *R*-matrix method has been used to perform a series of studies on low-energy electron–molecule collisions. These calculations are now capable of considering both subtle nuclear motion effects (Gillan *et al* 1987) and effects due to polarisation of the target charge cloud even at low scattering energies where these effects are most pronounced (Gillan *et al* 1988).

Over the last few years we have been using the molecular *R*-matrix method to study low-energy collisions between positrons and diatomic molecules (Tennyson 1986, Tennyson and Morgan 1987, Tennyson and Danby 1987, Danby and Tennyson 1988). These studies have produced a number of interesting results but have been uniformly defective in that the cross sections obtained at the lowest scattering energies were too low. We (Tennyson and Danby 1987) considered that this was due to the absence of intermediate-range polarisation effects which can be represented, within the *R*-matrix method, by the use of suitably chosen electronically excited states of the target. Use of these polarised pseudostates has been found to lead to a correct representation of the low-energy electron–N_2 cross section (Gillan *et al* 1988).

In this work we present a reformulation of the molecular *R*-matrix method for positrons which is computationally considerably more efficient than that previously implemented by Tennyson (1986). With this reformulation we present results for positron–hydrogen-molecule collisions using a variety of target representations and models for the collision process. The largest calculations involve using a fully correlated target, within a finite basis, and the representation of short-, intermediate- and long-range polarisation effects. The intermediate-range polarisation effects are represented using polarised pseudostates modelled on those used by Nesbet *et al* (1986) for electron–H_2 scattering calculations. In the course of implementing our new procedure a programming error was discovered which affected some of our previous positron scattering results. Corrected e^+–H_2 results are given here.

One advantage of the *R*-matrix method is that it is implemented in a general fashion which means that calculations are easily repeated for other diatomic targets and for a number of total symmetries. In this work we have used this feature to present differential cross sections for the e^+–H_2 collision process as a function of scattering energy.

2. Method

In earlier *R*-matrix studies of e^+–H_2 collisions (Tennyson 1986), the $X\,{}^1\Sigma_g^+$ target state was represented by a single configuration of molecular orbitals obtained from an SCF calculation. Occupied and virtual molecular orbitals were employed to account for correlation and polarisation effects within the region of space enclosed by a sphere centred on the molecular centre of mass. The coefficients of the resulting configuration expansion of the total positronic–electronic wavefunction were obtained by diagonalising the associated Hamiltonian matrix. From these one may obtain the amplitudes, on the surface of the *R*-matrix sphere, of the positronic continuum orbitals, which, together with the eigenvalues, yield the *R* matrix. This is matched to the solution, in the external region, of differential equations describing the motion of the positron in the quadrupolar field of H_2. The simple nature of the positron–molecule interaction beyond the target charge cloud allows *R*-matrix propagation and asymptotic series methods to be used.

Until recently (Danby and Tennyson 1990) all *R*-matrix calculations of positron–molecule collisions have been performed at the adiabatic fixed-nuclei level. In the present (as in the previous) work the protons are kept fixed at their equilibrium separation, R_e, though we note that at the non-adiabatic level, the inner region may be generalised to be a hypersphere in the configuration space of all (nuclei, electrons, positron) particles (Gillan *et al* 1987).

In addition to repeating calculations of the type just outlined, with improved algorithms, we have now included up to three multiconfiguration states of the H_2 target in the expansion of the total wavefunction. The generalisation of the electron–molecule theory to treat positron impact may be illustrated in five parts, corresponding to the computational procedure followed.

2.1. Target states and pseudostates

At the SCF level, molecular orbitals for the target wavefunction are constructed from a linear combination of Slater-type atom-centred orbitals (LCAO-STO). Two STO bases have been used in the present work. The ($1s\sigma$, $2s\sigma$, $2p\sigma$) basis of Fraga and Ransil (1961) (FR), extended to include ($2p\pi$, $3p\pi$, $3d\pi$) orbitals (Tennyson 1986), was chosen partly to correct our previous work (Armour 1988, table 9). More extensive calculations have been performed with the ($1s\sigma$, $1s\sigma$, $2p\sigma$, $2p\sigma$, $2p\pi$, $3p\pi$, $3d\pi$) basis developed by Nesbet *et al* (1986) (NNM) to account for H_2 polarisation in e^-–H_2 scattering. In our final calculations this basis has been augmented by a $3d\delta$ orbital whose exponent was arbitrarily set to that of the NNM $3d\pi$ orbital.

For consistency with previous work, calculations performed using the FR basis were performed with $R_e = 1.4\ a_0$ and those using NNM with $R_e = 1.402\ a_0$, although this difference is unlikely to be significant.

Whereas we only use FR basis for an SCF treatment of the ground state, that of NNM was additionally used to generate molecular orbitals for the construction of pseudostate, as well as ground-state, configurations. Specifically, occupied and virtual σ_g, π_u and π_g (and δ_g and δ_u where appropriate) molecular orbitals were taken from an SCF determination of the X $^1\Sigma_g^+$ state, a $^3\Sigma_u^+$ calculation providing those of σ_u symmetry. Following Nesbet *et al* a 'reduced CI' target was generated by diagonalising the Hamiltonian formed from the $1\sigma_g^2$, $1\sigma_u^2$ and $1\pi_u^2$ configurations with single configuration pseudostates represented by $1\sigma_g^1 1\sigma_u^1$ and $1\sigma_g^1 1\pi_u^1$. Full CI target and pseudostates were generated including all symmetry-allowed configurations. The total number of configurations of $^1\Sigma_g^+$, $^1\Sigma_u^+$ and $^1\Pi_u$ symmetry are, respectively, 32, 25 and 24 or 34, 26 and 30 with δ orbitals included.

Taking the lowest eigenstate from the CI calculation yields a representation of the ground state which recovers about 90% of the correlation energy and two pseudostates which act to account for the static polarisability. The inclusion of these diffuse pseudostates may be expected to lead to an improved description of the polarisation potential for e^+–H_2 collisions in (intermediate) regions of space within the R-matrix boundary but where the electron density of the ground target state is low.

In this work, in common with most previous molecular R-matrix calculations, the R-matrix radius was fixed at 10 a_0. Recent electron–H_2 studies (Branchett and Tennyson 1990) have shown that this sphere is more than adequate to contain the H_2 ground state but too small for some of the diffuse electronically excited states.

2.2. Continuum orbital generation

The first step in the generation of the continuum orbitals, which will carry the scattered positron, is the numerical solution, for each contributing partial wave l, of the differential equation in Ryd

$$\left(-\frac{d^2}{dr^2}+\frac{l(l+1)}{r^2}+V_0-k_{li}^2\right)u_{li}(r)=0 \tag{1}$$

with the reduced radial functions, u_{li}, satisfying the homogeneous boundary conditions

$$u_{li}(0)=0 \qquad \frac{a}{u_{li}(a)}\frac{du_{li}}{dr}\bigg|_{r=a}=0. \tag{2}$$

The basis generating potential, V_0, is in principle arbitrary and in most cases the reults are insensitive to it (Tennyson 1986). We therefore used $V_0 = 0$ for all calculations except for those giving continuum orbitals of π symmetry. These were generated using the isotropic electron–H_2 potential. The reasons for this seemingly unphysical choice will be discussed below.

A boundary value problem of the above (homogeneous Sturm–Liouville) type yields, for each l, an infinite orthonormal set of discrete eigenfunctions, though only those with $k_{lj}^2 \leq 10$ Ryd are retained. The effect of the neglected terms on the diagonal R-matrix elements may be taken into account by a Buttle correction (Buttle 1967, Shimamura 1978) evaluated at this stage of the calculation. Numerical functions were generated to represent the three lowest partial waves for each symmetry.

2.3. *Molecular integrals*

The numerical evaluation of the one- and two-electron integrals over the atom-centred STO and the continuum functions (centred on the molecular centre of mass) is performed at this stage using the program of Noble (1982) based on the ALCHEMY (McClean 1971) package. In earlier studies of positron–molecule scattering (Tennyson 1986) an independent set of STO was used in the construction of short-range positronic orbitals, even though in practice these were always taken to be identical to the occupied and virtual target orbitals. This method obviated the need for reprogramming to allow dual occupancy of spin orbitals. With these changes now made (see below), a significant reduction in the number of integrals to be calculated and stored has been effected, while retaining the previous approach as an option.

A fully orthonormal set of molecular orbitals is obtained using Schmidt orthogonalisation. This may be preceded by a Lagrange orthogonalisation of the continuum functions to a specified number of target molecular orbitals of the same symmetry, a procedure less prone to problems associated with linear dependence (Tennyson *et al* 1987). In the present work, the σ_g, σ_u, π_u and π_g continuum orbitals were Lagrange orthogonalised to the lowest target molecular orbital of the same symmetry. These molecular orbitals are used with a standard four-index transformation of the integrals between atomic basis functions to give molecular integrals.

2.4. *Hamiltonian matrix*

With the possible exception of the choice of the continuum basis generating potential, the procedure followed so far is the same whether the scattered particle is a positron or an electron. The calculations begin to differ when the target and continuum molecular orbitals are used to generate the configurations representing (for a given symmetry) the total wavefunction of the electrons and positron inside the R-matrix sphere:

$$\Psi_k(\boldsymbol{x}_1,\boldsymbol{x}_2,\boldsymbol{x}_3)=\sum_{ij}c_{ijk}\Phi_i(\boldsymbol{x}_1,\boldsymbol{x}_2)\eta_j(\boldsymbol{r}_3)\beta(\sigma_3)+\sum_i d_{ik}\phi_i(\boldsymbol{x}_1,\boldsymbol{x}_2)\phi_i'(\boldsymbol{r}_3)\beta(\sigma_3) \tag{3}$$

where $\boldsymbol{x}_i$ are the space-spin coordinates $(\boldsymbol{r}_i, \sigma_i)$ of the electrons $(i = 1, 2)$ and positron $(i = 3)$, β is the positron spin function and Φ_i is a target state or pseudostate consisting of a weighted sum of configurations determined in section 2.1. The choice of continuum molecular orbitals η_j is determined by the symmetry of the target state(s). The ϕ_i are short-range functions constructed from the target spin orbitals. In all configurations the target is explicitly coupled to a specific spin state, here a singlet.

With an SCF target two types of configurations are included in the second sum in (3). *Correlation* configurations $\Phi_i\phi'_i$ are included to allow for high-l effects in the region of the target singularities and to relax orthogonalisation constraints discussed above. *Polarisation* configurations can be included by considering single excitations out of the occupied orbitals with the positron occupying appropriate (by symmetry) ϕ'_i. The function of these *two-particle one-hole* states is to account for short-range polarisation effects. For CI targets the number of correlation configurations required increases, but it is no longer possible to distinguish these from polarisation configurations.

Expressions for the Hamiltonian matrix elements between the configurations generated above are evaluated in terms of a list of coefficients to be combined with that of the integrals obtained earlier. With each such coefficient is associated one label identifying the corresponding Hamiltonian matrix element and another the integral it multiplies (Yoshimine 1973, equation (3)). This is the point at which the bulk of the reprogramming was necessary in order to generalise the codes for positron collisions. The signs of the coefficients attached to the one-electron nuclear attraction integrals are changed, and two-electron exchange contributions neglected.

An error present in earlier implementations of the method (Tennyson 1986, Tennyson and Danby 1988, Danby and Tennyson 1988) led to the retention of some exchange contributions and the neglect of the corresponding positron–electron attraction terms. Previous e^+–molecule calculations beyond the static approximation were affected by this, and consequently some have been corrected in the present paper.

The occupation of electronic spin orbitals by the positron is most easily effected, not by changing the configuration generator (which in its original form enforces the Pauli principle), but by initially having separate positron spin orbitals (as in previous work) and *mapping* the integral label of each coefficient accordingly. After re-ordering this coefficient list to minimise input/output operations (Yoshimine 1973), it is combined with the list of integrals to yield the Hamiltonian matrix elements between configurations.

For a multiconfiguration (CI) target state the weight of each configuration is determined by performing a CI calculation for the target or pseudo-target state concerned, Φ_i. These weights are then used to transform the Hamiltonian matrix elements involving continuum orbitals. This contracted Hamiltonian is then diagonalised to yield the variational coefficients along with the eigenvalues, E_k, of Ψ_k. The differences between the eigenvalues and the energy of the lowest target state appear in the denominator of the R matrix at $r = a$ and hence are known as the R-matrix poles.

2.5. *Outer region*

The initial conditions for the solution of the scattering problem in the outer region of configuration space are provided by the R matrix on the surface of the sphere $r = a$ (taken in the present work as 10 a_0). Beyond the R-matrix sphere, the problem reduces to a set of close-coupled differential equations which must be solved for each energy E (Gillan *et al* 1987). A combination of R-matrix propagation (Morgan 1984) and (Gailitis) asymptotic expansion techniques (Noble and Nesbet 1984) was deployed. The (closed) pseudochannels were excluded and, instead, the asymptotic form of the polarisation potential adopted. Following Nesbet *et al* (1986), we used $(\alpha_{\parallel}, \alpha_{\perp}) = (6.2654, 4.3590)$ (units are a_0^3) for our calculations with a full CI target, and (6.2298, 4.4573) for 'reduced CI' calculations. The interaction with the H_2 quadrupole, taken from NNM as $Q = 0.447\ ea_0^2$, was also included. For positrons the polarisabilities give an attractive interaction and the quadrupole net repulsion.

3. Results

Preliminary to obtaining final results in this study we investigate the effect of the use of different target representations and ways of accounting for polarisation. For space reasons we only present detailed comparisons for the Σ_g^+ total symmetry although most models were tested for several symmetries.

Table 1 gives the behaviour of the eigenphase sum for four target representations as short- and long-range polarisation effects are included. The static calculations with the SCF Fraga–Ransil (FR) target are very similar to those given previously (Armour 1988, table 9, column 4) although they were generated on the Cray-XMP48 at the Atlas Laboratory using our new code. These static results are very similar to those given using an SCF target due to Nesbet *et al* (NNM).

Table 1. Σ_g^+ eigenphase sums, in rad, for positron–H_2 scattering as a function of a model using an SCF target wavefunction as described by FR (Fraga and Ransil 1961) or NNM (Nesbet *et al* 1986), and a full CI wavefunction using the NNM basis.

	Static		SP[a]			SP+α[b]			SP+α[b,c]	
k^2 (Ryd)	FR	NNM	FR	NNM	CI	FR	NNM	CI	NNM+δ	CI+δ
0.01	−0.072	−0.068	0.087	0.078	0.055	0.102	0.095	0.069	0.100	0.077
0.04	−0.142	−0.139	0.119	0.109	0.074	0.128	0.119	0.081	0.126	0.092
0.09	−0.209	−0.206	0.098	0.096	0.056	0.108	0.105	0.064	0.115	0.076
0.16	−0.274	−0.273	0.045	0.046	0.007	0.053	0.055	0.015	0.066	0.028
0.25	−0.336	−0.331	−0.022	−0.010	−0.046	−0.016	−0.003	−0.039	0.008	−0.027
0.36	−0.394	−0.371	−0.088	−0.056	−0.090	−0.083	−0.051	−0.081	−0.038	−0.071
0.49	−0.448	−0.425	−0.149	−0.120	−0.152	−0.145	−0.116	−0.148	−0.103	−0.135
0.64	−0.497	−0.487	−0.206	−0.183	−0.214	−0.203	−0.179	−0.210	−0.167	−0.197
0.81	−0.539	−0.522	−0.256	−0.208	−0.240	−0.253	−0.206	−0.237	−0.193	−0.223
1.00	−0.578	−0.563	−0.299	−0.240	−0.270	−0.296	−0.237	−0.267	−0.224	−0.253

[a] Static plus short-range polarisation.

[b] Static plus short- and long-range polarisation.

[c] Targets including δ orbitals.

Inclusion of short-range polarisation effects by use of single excitations in the target virtual orbitals leads to a significant increase in the Σ_g^+ eigenphase sum. The FR results presented here correct the equivalent results of Tennyson (1986, table 1 final column). Comparison between the FR and NNM SCF targets shows that the FR eigenphase sums are marginally higher at low energy and lower at high energy. A more significant difference is found when the NNM target is fully correlated. This leads to a significant decrease in the computed eigenphase sum at all energies. This can be explained by the improvement of the representation of the target relative to the continuum wavefunction which leads to an increase in the R-matrix pole positions and hence a lowering of the eigenphases. This suggests that it is in fact possible to overestimate the eigenphase sum by using a poor target representation, a phenomenon known as over-correlation.

The third set of columns in table 1 shows the effect of including the polarisabilities in the the asymptotic potential. As this term is attractive this leads to a near uniform rise in the eigenphase sum for all targets which is more significant at low scattering energies.

The final columns of table 1 show the effect of including a δ_g and a δ_u orbital in the target orbital set. This allows for Δ polarisation effects to be included as well as augmenting the Σ and Π polarisation. Inclusion of these single, arbitrarily defined, δ orbitals leads to a uniform increase in the eigenphase sums of about 0.014 rad. Again this effect is slightly less for the CI target because use of the extra orbitals also leads to a corresponding lowering of the energy of the full CI target. Nevertheless using these functions lead to a 15% increase in our final Σ_g cross section at 0.01 Ryd.

Table 2 investigates the effect of using polarised pseudostates to represent intermediate polarisation effects. For comparison the final column of table 1 and the best Kohn variational results, due to Armour and Baker (1986), are also given. These calculations, in common with others by Armour and co-workers, used a target representation which recovers about 50% of the H_2 correlation energy. Column 3 investigates the use of pseudostates generated following the prescription of NNM by using a three-configuration target representation and two single-configuration pseudostates. The poorness of these results can be attributed to both the crudeness of the pseudostates and the fact that this model leads to a large reduction in the number of configurations used to represent short-range polarisation effects.

Table 2. *R*-matrix Σ_g^+ eigenphase sums, in rad, for positron–H_2 scattering as a function of a model using CI target wavefunctions. Eigenphases obtained by Armour and Baker (1987) using Hylleraas functions and the Kohn variational principle are shown for comparison.

	SP+α[a]	SP+PSS+α[b]			Kohn
k^2 (Ryd)	CI+δ	NNM[c]	Full[d]	Full+δ[d,e]	type 1[f]
0.01	0.077	0.038	0.099	0.105	0.157
0.04	0.092	0.012	0.112	0.120	0.213
0.09	0.076	−0.035	0.086	0.096	0.199
0.16	0.028	−0.094	0.037	0.049	0.155
0.25	−0.027	−0.147	−0.007	0.005	0.066
0.36	−0.071	−0.184	−0.041	−0.028	−0.002
0.49	−0.135	−0.239	−0.094	−0.081	−0.058
0.64	−0.197	−0.297	−0.146	−0.133	
0.81	−0.223	−0.326	−0.164	−0.151	
1.00	−0.253	−0.360	−0.187	−0.173	−0.217

[a] Static plus short- and long-range polarisation.
[b] Static plus short-, intermediate- and long-range polarisation.
[c] Polarised pseudostates defined following Nesbet *et al* (1986).
[d] Polarised pseudostates defined using a full CI.
[e] Targets including δ orbitals.
[f] Column e, table 2 of Armour and Baker(1987).

The fourth column of table 2 shows that the use of full CI pseudostates with a full CI target leads to a significant rise in the eigenphase sum at all energies, demonstrating the importance of the intermediate-range polarisation effects. Comparison of these results with the Kohn calculations, employing Hylleraas functions to explicitly correlate the e^+–e^- motions, suggests that at low energies we are still underestimating the s-wave eigenphase. Some improvement is obtained by using δ orbitals; see column 5 of table 2. However it would appear that, particularly for the penetrating s wave, the polarisation potential is difficult to represent accurately without using Hylleraas functions. Conversely, at higher energies our eigenphase sums are higher than those given in the Kohn calculations. We attribute this to the inclusion of higher partial waves neglected by Armour and Baker who only allowed for the, albeit spheroidal, s wave in their calculations.

Table 3 gives eigenphase sums for the higher symmetries. These results were calculated using the full CI target including δ orbitals and pseudostates and are thus equivalent to column 5 of table 2. For comparison we also give the recent Σ_u^+ calculations of Armour *et al* (1989). Our results are in excellent agreement with theirs except at higher energies where our eigenphases are higher. Again this is probably due the inclusion of only the lowest partial wave in their calculation. The good agreement at low energies suggests that, although our polarisation potential is inadequate for the Σ_g^+ calculations, it can give reliable results for the higher symmetries which do not penetrate the target region so strongly.

Table 3. Eigenphase sums, in rad, for higher symmetry positron–H_2 scattering calculated using a full CI target with short-, intermediate- and long-range polarisation. The Kohn result due to Armour *et al* (1989) for Σ_u^+ symmetry is given for comparison.

k^2 (Ryd)	Σ_u^+	Σ_u^+ [a]	Π_u	Π_g	Δ_g	Δ_u
0.01	0.000	0.000	0.009	0.000	0.003	0.000
0.04	0.013	0.017	0.020	0.002	0.009	0.002
0.09	0.036	0.037	0.046	0.004	0.016	0.005
0.16	0.064	0.056	0.088	0.018	0.023	0.007
0.25	0.082	0.066	0.108	0.050	0.032	0.010
0.36	0.082	0.072	0.089	0.072	0.042	0.015
0.49	0.075	0.069	0.065	0.058	0.051	0.020
0.64	0.072	0.063	0.067	0.027	0.060	0.026
0.81	0.080	0.050	0.094	0.019	0.071	0.032
1.00	0.131	0.041	0.126	0.057	0.081	0.042

[a] Armour *et al* (1989) table 4, final column. The *R*-matrix results quoted by these authors are our preliminary values which did not include δ orbitals in the calculation.

Our results suggest that the Π_u symmetry is more important at low energies than the Σ_u^+ symmetry, as anticipated by Armour *et al.* Our calculations on the Δ symmetries give eigenphase sums that are small, positive and monotonically increasing—in line with calculations of the d-wave contribution to e^+–He scattering (Campeanu 1977).

For both Π_u and Π_g symmetries, our results showed a pronounced dip in the eigenphase sums in the region 0.4–0.8 Ryd. We could find no obvious physical explanation for this effect. Therefore we performed several test calculations to probe the cause of this effect. The magnitude of the dip was found to be much more sensitive to the details of the calculation than, for instance, the eigenphases with Σ or Δ symmetry.

In particular the Π eigenphases appeared to depend strongly on both the exact form of the continuum numerical functions and the level of short-range polarisation included in the calculation. So, for example, the Π_u eigenphase sum for $k^2 = 0.081$

Ryd increased 0.021 rad when d orbitals were used. This is 50% larger than any of the increases for other symmetries.

The sensitivity to choice of continuum functions appears to be more of a technical problem. Unfortunately the Π target orbitals developed by Nesbet *et al* (1986) are themselves nearly linearly dependent. When these are augmented by a set of continuum functions a linear dependence occurs which is not well treated by our Lagrange orthogonalisation procedure (Tennyson *et al* 1987) as the underlying cause of it is the target and not the continuum orbitals. This results in an underestimate of the eigenphase sums in calculations using Lagrange orthogonalised orbitals. Numerical experimentation showed that this effect was least severe for continuum functions which *maximised* the overlap with the target orbitals. Hence the choice of the attractive *electron*–H_2 potential for generating our continuum orbitals.

Table 4 presents cross sections calculated using the results of table 3 and column 4 of table 2. The total cross sections are too small when compared with experiment (Hoffman *et al* 1982, Charlton *et al* 1983) which can be directly attributed to our underestimate of the Σ_g^+ contribution. Our total cross sections are compared with those obtained by Nesbet *et al* (1986) for e^-–H_2 scattering showing the much larger cross section in the electron case. Comparison with experiment (Hoffman *et al* 1982) shows that these calculations also underestimate the total cross section at the lowest scattering energies.

Table 4. Cross sections, in a_0^2, for positron–H_2 scattering calculated using a full CI target with short-, intermediate- and long-range polarisation. The Kohn results for Σ_g^+ and Σ_u^+ symmetry are given for comparison, as is the calculated total electron–H_2 cross section.

k^2 (Ryd)	Σ_g^+	Σ_g^+ [a]	Σ_u^+	Σ_u^+ [b]	Π_u	Π_g	Δ_g	Δ_u	Total(e^+)	Total(e^-)[c]
0.01	13.967	30.744	0.003	0.000	0.219	0.002	0.031	0.001	14.22	37.80
0.04	4.321	13.986	0.053	0.089	0.237	0.003	0.052	0.003	4.67	43.58
0.09	1.076	5.448	0.166	0.186	0.518	0.005	0.062	0.005	1.83	48.26
0.16	0.111	1.885	0.281	0.249	1.069	0.044	0.068	0.007	1.58	52.69
0.25	0.066	0.232	0.273	0.218	0.998	0.222	0.080	0.008	1.65	54.07
0.36	0.263	0.000	0.170	0.178	0.431	0.316	0.092	0.011	1.28	51.21
0.49	0.495	0.085	0.088	0.121	0.126	0.137	0.096	0.015	0.97	45.38
0.64	0.801		0.052	0.079	0.096	0.015	0.100	0.018	1.08	39.01
0.81	0.989		0.046	0.041	0.152	0.005	0.106	0.022	1.32	33.64
1.00	1.036	0.581	0.109	0.027	0.220	0.048	0.108	0.031	1.55	25.85

[a] Armour and Baker (1987) table 5, column (b).

[b] Armour *et al* (1989) table 5, final column.

[c] Electron–H_2 cross sections from Nesbet *et al* (1986).

Figure 1 shows the convergence of a calculation of the e^+–H_2 differential cross section as a function of the number of symmetries. Although the shape of the curves changes markedly as symmetries are included, the small change on including the Δ_u symmetry suggests that our results are converged at this level.

Figure 2 shows differential cross sections as a function of scattering energy. A notable feature of this figure is the prediction of a minimum in the differential cross sections for an angle of about 45° for scattering energies between 0.3 and 0.6 Ryd. This feature is very similar to that predicted in low-energy e^+–He scattering (Campeanu 1977, Humberston 1979), but the larger total cross section of the e^+–H_2 system makes it a more promising candidate for observation. A similar feature was found in the

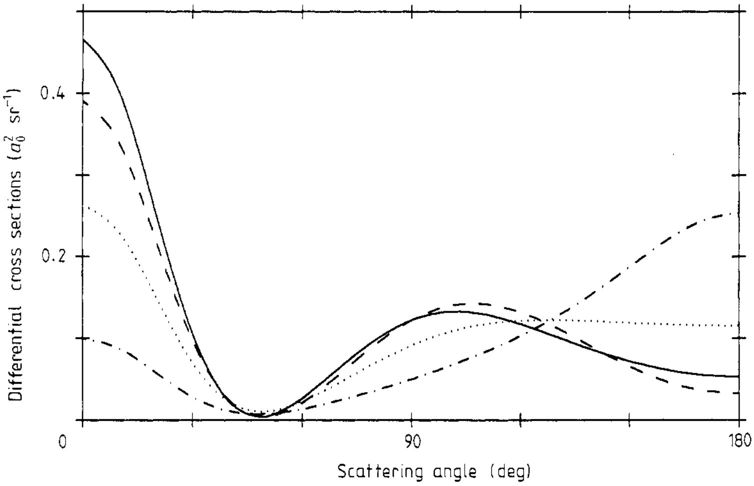

Figure 1. Differential cross sections for e^+–H_2 collisions at 0.5 Ryd as a function of number of symmetries included in the calculation. Symmetries are included in the order $\Sigma_g^+, \Sigma_u^+, \Pi_u, \Pi_g, \Delta_g$ and Δ_u. Chain curve, three symmetries; dotted curve, four symmetries; broken curve, five symmetries; full curve, six symmetries.

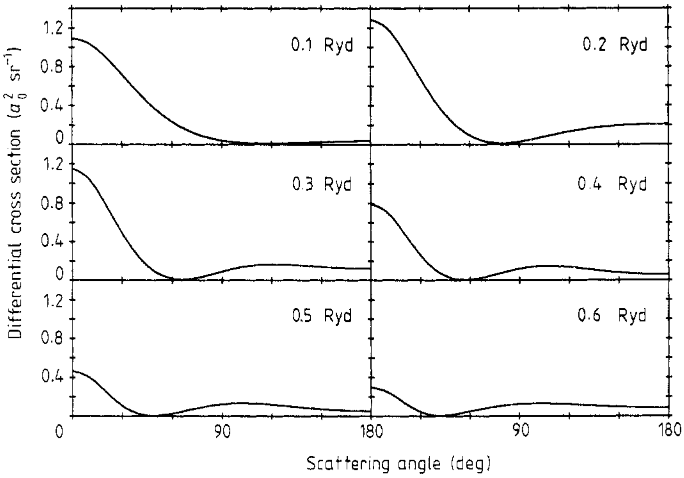

Figure 2. Differential cross sections for e^+–H_2 collisions as a function of collision energy. The results include all symmetries up to and including Δ_u.

model potential calculations of Morrison *et al* (1984), although their differential cross sections appear to be significantly more forward peaked. As the Σ_g cross sections are forward peaked for all but the lowest energies, our underestimate of this cross section will act to lower this peak. At higher energies, one would expect symmetries higher than Δ_u to also make a significant contribution to the forward cross section.

4. Conclusions

We have presented results for positron–hydrogen molecule collisions using a number of target representations and different models for polarisation effects. These results show the importance of including short-, intermediate- and long-range polarisation effects. Our best results give eigenphase sums which are too low for the penetrating Σ_g^+ symmetry. This results in an underestimate of the low-energy cross section by up to a factor of two suggesting that our short-range representation of polarisation is still inadequate for this symmetry. These effects appear less important for the higher symmetries for which our results appear more reliable although we had some problems of a technical nature with the calculations of Π symmetry.

Our predicted differential cross sections show a structure similar to that found in some positron–atom systems. We believe this structure may be observable with present-day experimental techniques.

The improved formulation of the positron–molecule scattering problem presented in this paper makes possible calculations on a number of diatomic targets at the same level of sophistication as those presented here. Such calculations are currently in progress and it is our aim to study both elastic and inelastic processes in these works.

Acknowledgments

We would like to thank Lesley Morgan for many helpful discussions during the course of this work, and Edward Armour and Martin Plummer for communicating their results prior to publication. This work was performed under Science and Engineering Research Council grant GR/D/77414.

References

Armour E A G 1985 *J. Phys. B: At. Mol. Phys.* **18** 3361–8
—— 1988 *Phys. Rep.* **169** 1–98
—— 1989 *Comment. At. Mol. Phys.* **22** 173-84
Armour E A G and Baker D J 1987 *J. Phys. B: At. Mol. Phys.* **20** 6105–19
Armour E A G, Baker D J and Plummer M 1989 *J. Phys. B: At. Mol. Opt. Phys.* **22** 3097-108
Branchett S E and Tennyson J 1990 to be published
Buttle P J A 1967 *Phys. Rev.* **160** 719–29
Campeanu R I 1977 *PhD Thesis, University of London*
Charlton M 1985 *Rep. Prog. Phys.* **48** 737–93
Charlton M, Griffith T C, Heyland G R and Wright G L 1983 *J. Phys. B: At. Mol. Phys.* **16** 323–41
Danby G and Tennyson J 1988 *Phys. Rev. Lett.* **61** 2737–9
—— 1990 in preparation
Fraga S and Ransil B 1961 *J. Chem. Phys.* **35** 1967–77
Gillan C J, Nagy O, Burke P G, Morgan L A and Noble C J 1987 *J. Phys. B: At. Mol. Phys.* **20** 4585–603
Gillan C J, Noble C J and Burke P G 1988 *J. Phys. B: At. Mol. Opt. Phys.* **21** L53–9
Hoffman K R, Dababneh M S, Hsieh Y-F, Kauppila W E, Pol V, Smart J H and Stein T S 1982 *Phys. Rev.* A **34** 2798–808
Humberston J W 1979 *Adv. At. Mol. Phys.* **15** 101–33
Kauppila W E and Stein T S 1987 *Atomic Physics with Positrons* ed E A G Armour and J W Humberston (New York: Plenum) pp27–39
McClean A D 1971 *Conf. Potential Energy Surfaces in Chemistry* ed W A Lester Jr (San Jose: IBM Research Laboratory) p 87
Morgan L A 1984 *Comput. Phys. Commun.* **31** 419–22

Morrison M A, Gibson T L and Austin D 1984 *J. Phys. B: At. Mol. Phys.* **17** 2725–45
Nesbet R K, Noble C J and Morgan L A 1986 *Phys. Rev.* A **34** 2798–808
Noble C J 1982 *Daresbury Laboratory Technical Memorandum DL/SCI/TMT33T*
Noble C J and Nesbet R K 1984 *Comput. Phys. Commun.* **33** 399–411
Shimamura I 1978 *Electronic and Atomic Collisions* ed G Watel (Amsterdam: North-Holland) pp213–30
Tennyson J 1986 *J. Phys. B: At. Mol. Phys.* **19** 4255–63
Tennyson J, Burke P G and Berrington K A 1987 *Comput. Phys. Commun.* **47** 207–16
Tennyson J and Danby G 1987 *Atomic Physics with Positrons* ed E A G Armour and J W Humberston (New York: Plenum) pp111–21
Tennyson J and Morgan L A 1987 *J. Phys. B: At. Mol. Phys.* **20** L641–6
Ward S J, Horbatsch M, McEachran R P and Stauffer A D 1988 *J. Phys. B: At. Mol. Opt. Phys.* **21** L611–6
—— 1989 *J. Phys. B: At. Mol. Opt. Phys.* **22** 1845–61
Yoshimine M 1973 *J. Comput. Phys.* **11** 449–54